Electronic Supplementary Material (ESI) for Physical Chemistry Chemical Physics.
This journal is © the Owner Societies 2017

Supporting Information

Alkaline-Earth Metal (Mg) Polynitrides at High Pressure as a Possible High-Energy Material

*Shuli Wei, Da Li, Zhao Liu, Xin Li, Fubo Tian, Defang Duan, Bingbing Liu and Tian Cui**

*State Key Laboratory of Superhard Materials, College of Physics, Jilin University, Changchun, 130012, P. R. China. *Email: cuitian@jlu.edu.cn*

Index

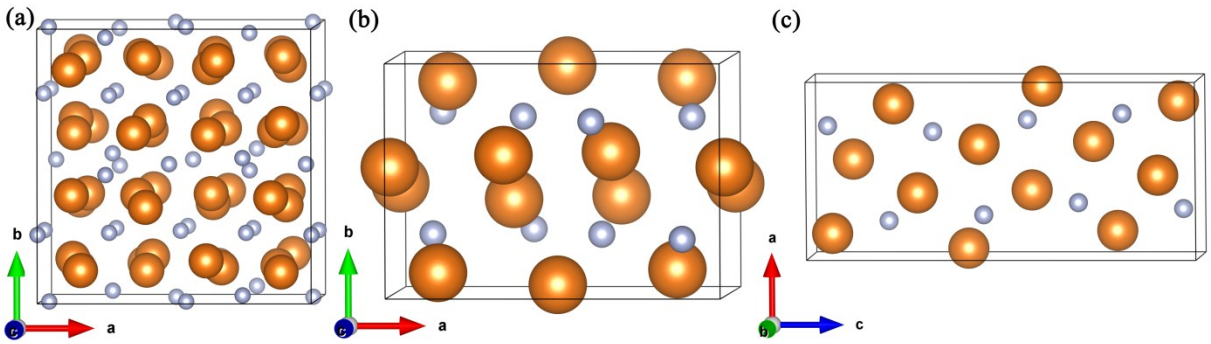

Figure. S1. Structures of stable Mg_2N_3 crystals: (a) *Ia*-3-phase at ambient pressure, (b) *Pbcn*-phase at 20 GPa and (c) *Pnma*-phase at 40 GPa.

Computational Details

Our structural prediction approach is based on a global minimization of free energy surfaces merging ab initio total-energy calculations with CALYPSO (Crystal structure AnaLYsis by Particle Swarm Optimization) methodology as implemented in the CALYPSO code. In the first step, random structures with certain symmetry are constructed in which atomic coordinates are generated by the crystallographic symmetry operations. Local optimizations using the VASP code were done with the conjugate gradients method and stopped when enthalpy changes became smaller than 1×10^{-5} eV per cell. After processing the first generation structures, 60% of them with lower enthalpies are selected to construct the next generation structures by PSO (Particle Swarm Optimization). 40% of the structures in the new generation are randomly generated. A structure fingerprinting technique of bond characterization matrix is applied to the generated structures, so that identical structures are strictly forbidden. These procedures significantly enhance the diversity of the structures, which is crucial for structural global search efficiency. In most cases, structural searching simulations for each calculation were stopped after generating 1000 ~ 1200 structures (e.g., about 20 ~ 30 generations).

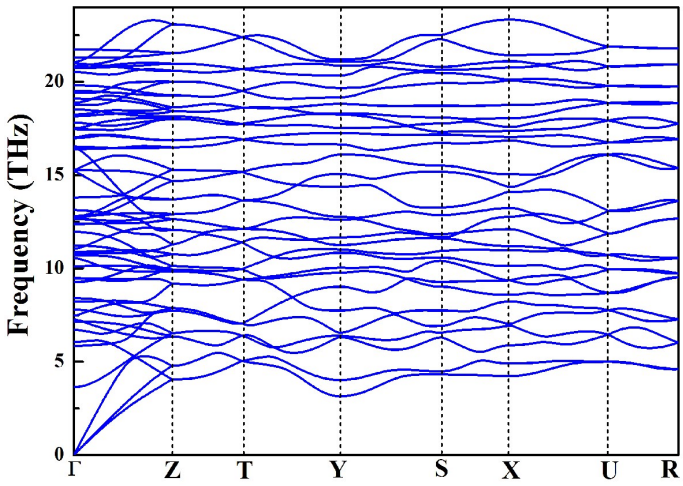

Figure. S2. Phonon dispersion curves of *Pbcn*-Mg_3N_2 phase at 20 GPa.

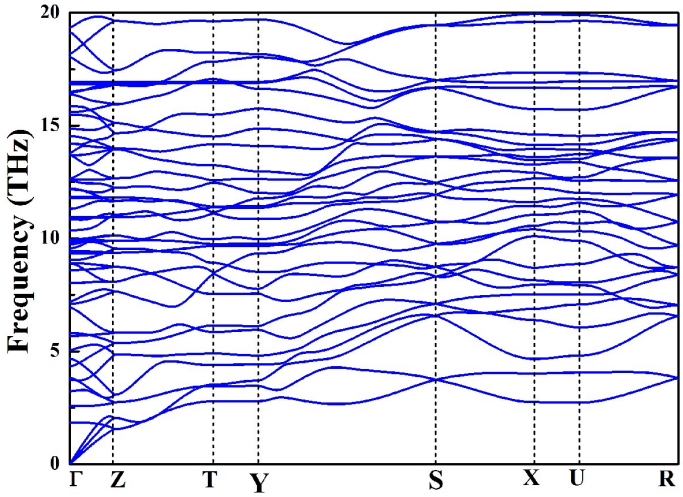

Figure. S3. Phonon dispersion curves of Pmma-Mg_3N_2 phase at 40 GPa.

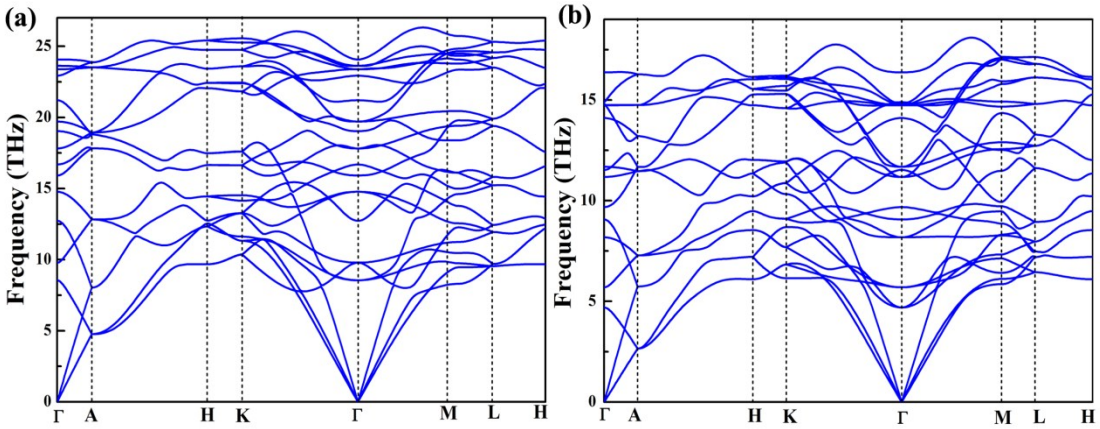

Figure. S4. Phonon dispersion curves of *P*6$_3$/*mmc*-MgN phase at 80 GPa (a) and 0 GPa (b).

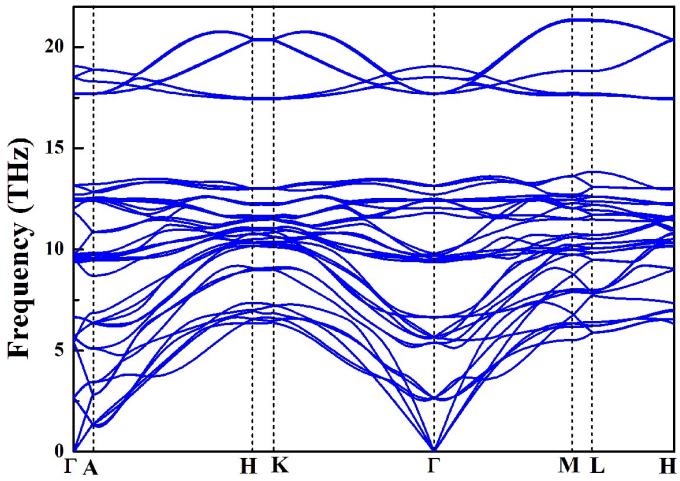

Figure. S5. Phonon dispersion curves of *R*-3*m*-Mg_2N_3 phase at 10 GPa.

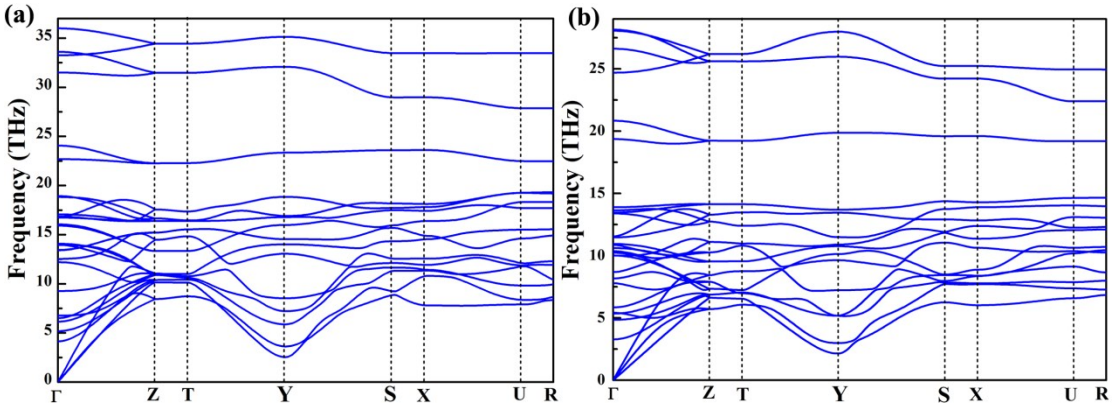

Figure. S6. Phonon dispersion curves of *Imm*2-Mg_2N_3 phase at 40 GPa (a) and 0 GPa (b).

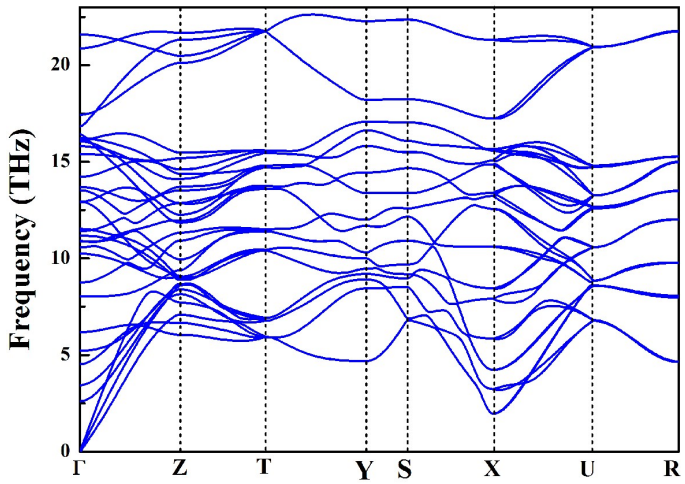

Figure. S7. Phonon dispersion curves of *Cmcm*-MgN_2 phase at 10 GPa.

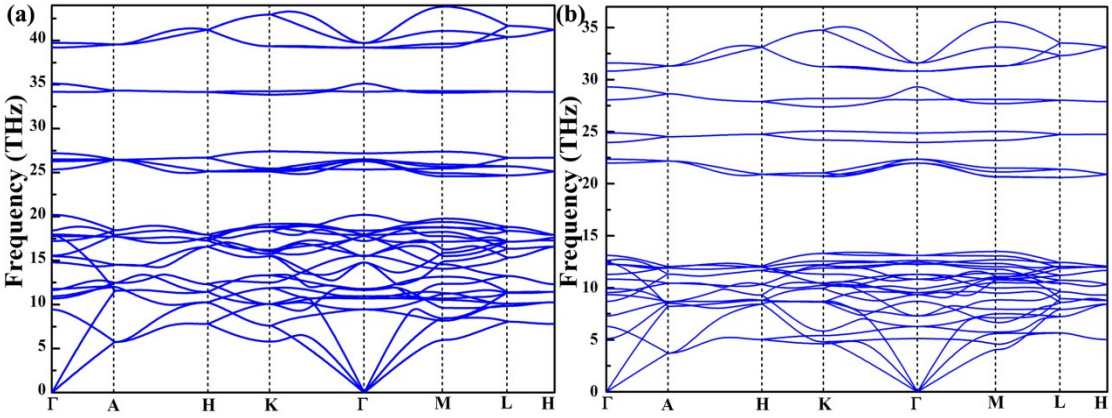

Figure. S8. Phonon dispersion curves of $P6_3/mcm$-MgN_2 phase at 60 GPa (a) and 0 GPa (b).

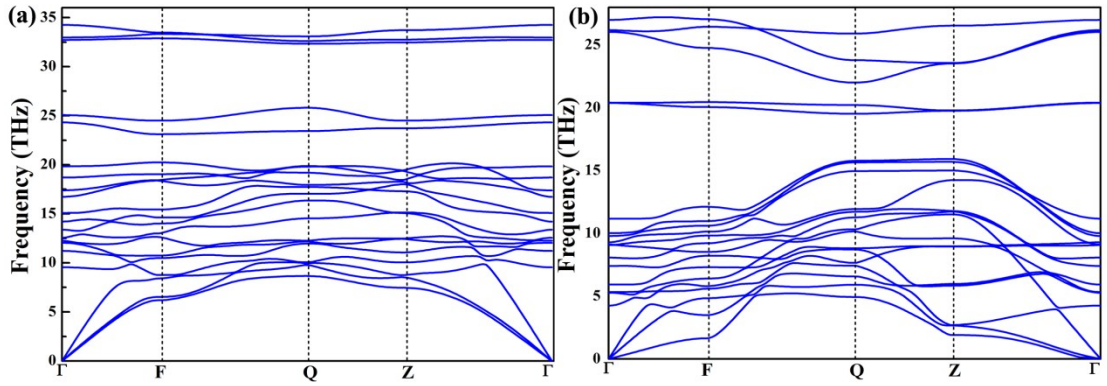

Figure. S9. Phonon dispersion curves of P-1-MgN_3 phase at 80 GPa (a) and 0 GPa (b).

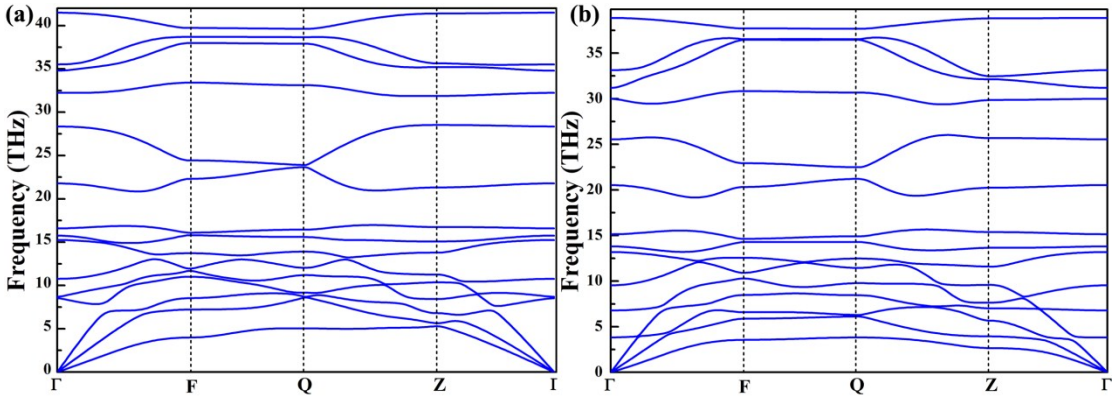

Figure. S10. Phonon dispersion curves of P-1-MgN_4 phase at 10 GPa.

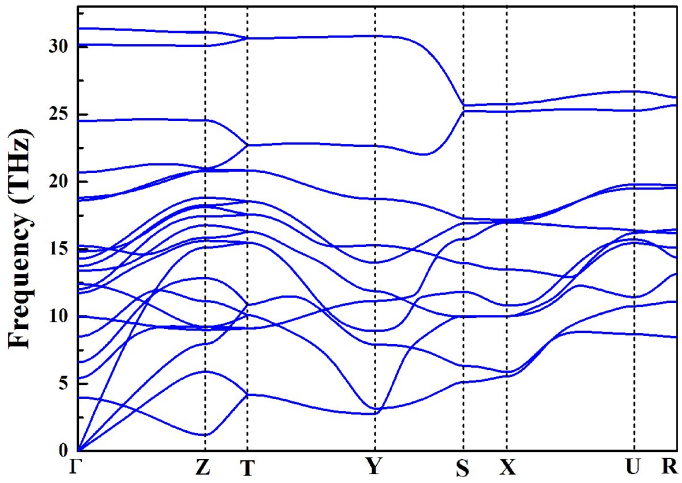

Figure. S11. Phonon dispersion curves of *Cmmm*-MgN_4 phase at 60 GPa.

Table S1. Structural parameters of all considered structures for Mg-N.

Str. And S.G.	Lattice parameters (Å, °)	Atomic coordinates (fractional)	Sites
***Ia*-3-Mg_3N_2** **P = 0 GPa**	a = 10.010 b = 10.010 c = 10.010	N1 (0.969, 0.0, 0.25) N2 (0.25, 0.25, 0.25) Mg (0.389, 0.153, 0.382)	24*d* 8*b* 48*e*
***Pbcn*-Mg_3N_2** **P = 30 GPa**	a = 7.363 b = 5.148 c = 5.249	N (0.115, 0.253, 0.532) Mg1 (0.652, 0.606, 0.609) Mg2 (0.5, 0.048, 0.75)	8*d* 8*d* 4*c*
***Pnma*-Mg_3N_2** **P = 40 GPa**	a = 5.554 b = 3.090 c = 12.191	N1 (0.187, 0.25, 0.193) N2 (0.245, 0.75, 0.450) Mg1 (0.360, 0.25, 0.561) Mg2 (0.533, 0.25, 0.103) Mg3 (0.632, 0.25, 0.720)	4*c* 4*c* 4*c* 4*c* 4*c*
***P*6$_3$/*mmc*-MgN** **P = 0 GPa**	a = 3.326 c = 8.604 γ = 120	N1 (0.667, 0.333, 0.354) Mg1 (0.0, 0.0, 0.0) Mg2 (0.667, 0.333, 0.57)	4*f* 2*a* 2*c*
***R*-3*m*-Mg_2N_3** **P = 20 GPa**	a = 2.952 c = 18.983 γ = 120	N1 (0.667, 0.333, 0.865) N2 (0.333, 0.667, 0.667) Mg (0.0, 0.0, 0.725)	6*c* 3*a* 6*c*
***Imm*2-Mg_2N_3** **P = 0 GPa**	a = 9.744 b = 2.985 c = 3.307	N1 (0.372, 0.0, 0.547) N2 (0.5, 0.0, 0.337) Mg (0.648, 0.5, 0.034)	4*c* 2*b* 4*c*
***Cmcm*-MgN_2** **P = 0 GPa**	a = 3.999 b = 8.574 c = 3.449	N1 (0.842, 0.893, 0.75) Mg (0.0, 0.368, 0.25)	8*g* 4*c*
***P*6$_3$/*mcm*-MgN_2** **P = 0 GPa**	a = 4.825 c = 5.527 γ = 120	N1 (0.0, 0.280, 0.75) N2 (0.0, 0.0, 0.75) Mg (0.667, 0.333, 0.5)	6*g* 2*a* 4*d*
***P*-1-MgN_3** **P = 0 GPa**	a = 5.267 b = 5.271 c = 3.025 α=85.72 β=86.01 γ=60.13	N1 (0.826, 0.303, 0.016) N2 (0.697, 0.131, 0.986) N3 (0.870, 0.828, 0.967) Mg (0.666, 0.667, 0.499)	2*i* 2*i* 2*i* 2*i*
***P*-1-MgN_4** **P = 0 GPa**	a = 3.218 b = 3.860 c = 4.191 α=101.20 β=84.05 γ=69.99	N1 (0.419, 0.982, 0.145) N2 (0.561, 0.373, 0.844) Mg (0.0, 0.0, 0.5)	2*i* 2*i* 1*g*
***Cmmm*-MgN_4**	a = 7.523	N (0.332, 0.316, 0.5)	8*g*

P =60 GPa	b = 3.589 c = 2.520	Mg (0.0, 0.5, 0.0)	2*b*

Table S1. Calculated Bader charges for *Imm*2-Mg_2N_3, *P*6_3/*mcm*-MgN_2, *P*-1-MgN_3 and *P*-1-MgN_4, respectively.

Str.	Atom	N	Charge value(e)	δ(e)
P6_3/*mmc*- MgN	Mg1	2	0.38	-1.62
	Mg2	2	0.39	-1.61
	N1	2	6.67	1.67
	N2	2	6.56	1.56
*Imm*2-Mg_2N_3	Mg	4	0.40	-1.60
	N1	4	6.31	1.31
	N2	2	5.58	0.58
P6_3/*mcm*-MgN_2	Mg	4	0.41	-1.59
	N1	2	4.97	-0.03
	N2	6	6.07	1.07
P-1-MgN_3	Mg	2	0.40	-1.60
	N1	2	5.55	0.55
	N2	2	5.53	0.53
	N3	2	5.52	0.52
P-1-MgN_4	Mg	1	0.37	-1.62
	N1	2	5.33	0.33
	N2	2	5.48	0.48

The discussion about the stabilities of predicted *P*-1-MgN_3 and *P*-1-MgN_4

The accuracy of searching crystal structure results by CALYPSO is lower than that of structural optimization results of DFT. To further analyze the structures with higher accuracy, we select a number of structures with lower enthalpies and perform structural optimization using density functional theory within the generalized gradient approximation as implemented in the VASP code. We have discussed the stabilities of predicted magnesium polynitirdes by comparing between CALYPSO crystal structure searching results and calculation results of DFT in the revised paper (see (see the Supporting Information, Fig. S1)). The phonon band dispersion for the *P*-1-MgN_3 predicted at 100GPa and the *P*-1-MgN_4 predicted at 20GPa shows the stabilities of predicted magnesium polynitirdes. To determine the transition pressure, the enthalpy curves of the predicted structures relative to the *P*-1-MgN_3 and *P*-1-MgN_4 have been plotted in Fig. 2. Clearly, the searching structure at special pressure point is still stable in the neighboring pressure range after structural optimization.

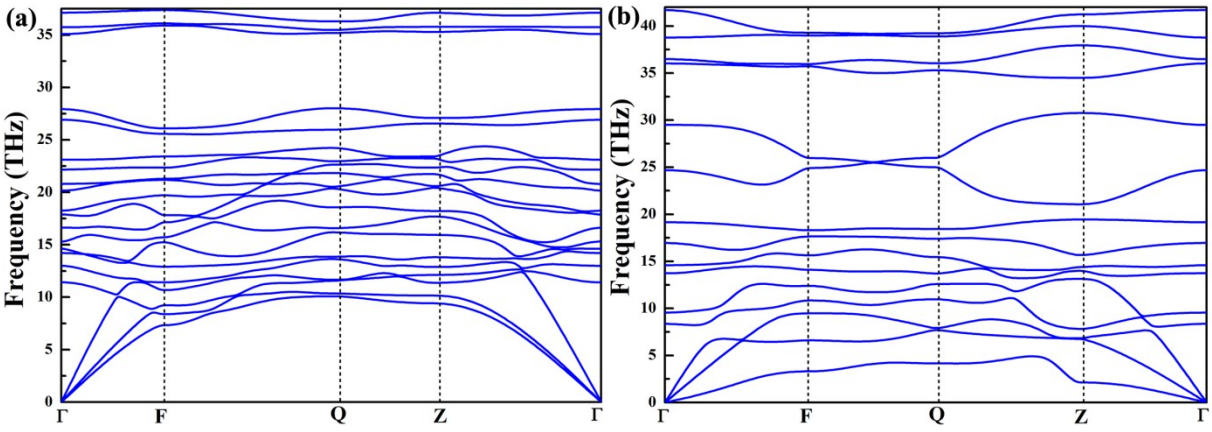

Figure. S12. Phonon dispersion curves of *P*-1-MgN_3 phase predicted at 100GPa and the *P*-1-MgN_4 phase predicted at 20GPa.

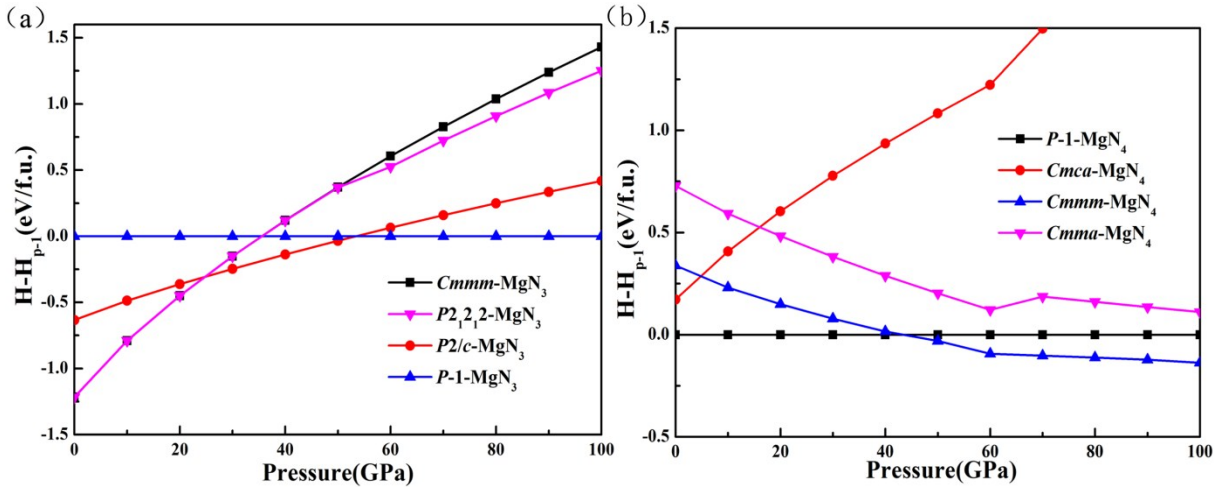

Figure. S13. (a) Enthalpy of the *Cmmm*-MgN_3, $P2_12_12$-MgN_3 and *P*2/*c*-MgN_3 phases relative to *P*-1-MgN_3 with pressure. (b) Enthalpy of the *Cmca*-MgN_4, *Cmmm*-MgN_4, and *Cmma*-MgN_4 phases relative to *P*-1-MgN_3 with pressure.